Max-Planck-Institut

für

Astrophysik

Annual Report 1995

The cover shows the present-day distribution of dark matter in a computer simulation of the growth of structure. This was the first scientific calculation carried out on the new Garching T3D parallel supercomputer. It integrated the equations of motion of 16,777,216 particles interacting through gravity and is the largest high resolution cosmological simulation so far carried out in Europe. The picture shows a thin slice through the simulation containing 6% of the total volume. The region is about one billion light years across. The smallest visible objects correspond to an isolated galaxy like our Milky Way, and the largest to a rich galaxy cluster. (For more information, see Sect. 2.11 in this report)

Annual Report of the Max-Planck-Institut für Astrophysik,
Postfach 1523, D–85740 Garching, Federal Republic of Germany.

Editors: H.-Th. Janka and S.D.M. White.

Printed by Dokumentationsstelle of the MPI für Astrophysik, Garching.

ISSN 0948–9525

Contents

1 General Information

1.1 A brief overview of the MPA

The Max-Planck-Institut für Astrophysik, usually called the MPA for short, is one of more than 70 autonomous research institutes within the Max-Planck Society. These institutes are primarily devoted to fundamental research. Most of them carry out work in several distinct areas, each led by a senior scientist who is a “Scientific Member” of the Max-Planck Society. The MPA was founded in 1958 under the direction of Ludwig Biermann. It was an offshoot of the MPI für Physik which at that time had just moved from Göttingen to Munich. In 1979 the headquarters of the European Southern Observatory (ESO) came to Munich from Geneva, and as part of the resulting reorganisation the MPA (then under its second director, Rudolf Kippenhahn) moved to a new site in Garching, just north of the Munich city limits. The new building lies in a research park barely 50 metres from ESO headquarters and is physically connected to the buildings which house the MPI für Extraterrestrische Physik (the “MPE”). This park also contains two other large research institutes, the MPI für Plasmaphysik and the MPI für Quantenoptik, as well as many of the scientific and engineering departments of the Technische Universität München (the “TUM”). The third and current director of the MPA is Simon White who took up the post in 1994.

Research at MPA is devoted to a broad range of topics in theoretical astrophysics. Major concentrations of interest lie in the areas of stellar evolution, stellar atmospheres, supernova physics, astrophysical fluid dynamics, high energy astrophysics, galaxy structure and evolution, the large-scale structure of the Universe, and cosmology. The MPA has traditionally been strong in studies of General Relativity, but in mid-1995 most of our relativity group moved to the newly founded MPI für Gravitationsphysik in Potsdam near Berlin. Their departure will allow a consolidation of MPA activities in extragalactic astrophysics, as well as an expansion in a new area, high energy astrophysics. While most MPA research addresses theoretical issues, the neighbouring institutes provide complementary expertise and there are many collaborative projects with them. The major research programmes at MPE are concerned with instrumental and observational aspects of infrared, X-ray and gamma-ray astronomy, together with supporting theoretical work, while ESO groups carry out a broad range of instrumental and observational projects in the optical and infrared wavebands.

At any given time the MPA has about 30 scientists working on long-term positions at postdoctoral level and above, up to 10 foreign visitors brought in for periods of varying length under a vigorous visitor programme, and about 20 graduate students. The students are almost all enrolled for degrees in one of the two large universities in Munich, the TUM and the Ludwig-Maximilians-Universität (LMU). A number of the senior staff at MPA have teaching affiliations with one or other of these universities. Ties with the Institute of Astronomy and the Observatory of the LMU are particularly close because the observatory director (Rolf-Peter Kudritzki) is also a Scientific Member of the MPA.

A recent development which should also enhance interactions with other local institutions is the approval by the German Science Foundation of a large long-term research programme on astro-particle physics (a “Sonderforschungsbereich der Deutschen Forschungsgemeinschaft”). Funding started in 1995 and is expected to continue for up to ten years. Participants in the programme include the physics departments of the two universities, the observatory of the LMU, the MPI für Physik, and the MPA.

1.2 Current MPA facilities

The MPA building itself is a major asset for its research activities. It was specially designed by the same architect as ESO headquarters, and the two buildings are generally considered as important and highly original examples of the architecture of their period. Although the unconventional geometry of the MPA can easily confuse first-time visitors, its open and centrally focussed plan is very effective at encouraging interaction between scientists and makes for a pleasant and stimulating research environment. Part of the ground floor and most of the basement of the building is currently occupied by the infrared group of the MPE, and this proximity significantly enhances the possibilities for interaction with this large and active observational/instrumental group.

The MPA and the MPE share a large and fully stocked astronomical library which is housed in the MPA building. All major astronomical books and periodicals are available. The library staff can also provide access to a variety of online archives and are currently extending this capability. Further library material is available at ESO which in addition maintains a complete collection of optical sky maps and photographic sky surveys. Other large data analysis facilities are available at the MPE which is the European data centre for the ROSAT satellite and is providing a data centre for the ISO satellite mission.

The MPA has always placed considerable emphasis on computational astrophysics and has therefore ensured access to forefront computing facilities. The current in-house system is based on a central cluster of about 10 IBM RS6000 workstations, with additional SGI graphics workstations for graphics applications. Users have free access to all workstations and are in general connected via large-screen X-window terminals or desk-top workstations. For larger computing tasks MPA scientists use the facilities of the central computing centre of the Max-Planck Society (known as the RZG). This is part of the MPI für Plasmaphysik and is located a few hundred metres from the MPA. Current facilities at the RZG include a 4-processor Cray YMP, a 16-processor Cray Jedi, a large cluster of high-end workstations and a Terabyte mass storage system. A new parallel machine, a 128 processor Cray T3D arrived in 1995, it will be upgraded to a 400 processor T3E during 1996. MPA scientists have free access to the RZG and are among the top users of the facilities there. An AFS file system ensures that the transfer of data among the MPA machines and from MPA to the RZG is now almost transparent to the user. Further computing power is available at a second Max-Planck Society computer centre which is operated jointly with the University of Göttingen, and provides additional access to large parallel machines.

1.3 1995 at the MPA

1995 saw a number of changes at the MPA. One of the most far-reaching was the departure of our General Relativity group to found the new MPI für Gravitationsphysik under the leadership of Jürgen Ehlers. They left Garching at the end of the Spring, throwing a memorable goodbye party for the rest of the MPA. Rumours from Potsdam say that things are going well at their new home even though they don't yet have their new building or their full quota of directors. Their departure should, in principle, have reduced the pressure on office space in the MPA building, but in practice new developments led to expansion in other areas which meant that desks for visitors were in very short supply by the end of the year.

A major new development was the appointment of Rashid Sunyaev as a full-time Scientific Member at the MPA which took effect at the beginning of October. He and his family moved to Munich in the latter part of the year and he is currently starting up a new high energy astrophysics group at the MPA while at the same time maintaining all the satellite projects which he leads at the Space Research Institute in Moscow. This is not a simple task in the face of the rapidly changing scientific situation in Russia, and requires frequent use of the excellent airline connections between Munich and Moscow.

The arrival of R. Sunyaev completes the currently expected additions to MPA staff at Scientific Member level, and ensures a substantial growth in our activity in high energy astrophysics in the next few years. It also makes it possible to start implementing a long planned change in the management structure of the MPA, namely the switch from the current system in which a single Director manages the institute on a permanent basis to one in which the full-time Scientific Members form a Board of Directors and the role of Managing Director rotates among them. This system is the one currently employed at almost all other Max-Planck Institutes and has the great advantage of sharing the management duties more evenly among the senior scientists. The implementation of the new structure should be complete by the end of 1996.

As usual 1995 saw a large number of scientists passing through the MPA to give talks, for short-term collaborative visits, or for longer stays as part of our visitor programme. A new source of visitors is a regular weekly Joint Astronomy Colloquium which is co-organised by the MPA, the MPE, ESO and the LMU observatory. This series began with the New Year, bringing in Wendy Freedman to present results from the Hubble Space Telescope Key Project to determine the extragalactic distance scale. Since then a steady stream of high profile invitees and of excellent talks have kept the ESO auditorium consistently near capacity and have established the JAC as a regular feature of astronomical life in Garching.

Institutional collaboration with the other Garching institutes has continued in other ways. ESO and MPA jointly organised a three-day workshop in June on "Spiral Galaxies in the Infrared". This attracted more than 60 participants, including quite a number of scientists from the MPE infrared group. A growing MPA interest in observational work was also signaled by our hosting of a two-day meeting of the international Theory Working Group which has been helping to write the scientific case for the COBRAS/SAMBA satellite. This case will be presented to the ESA community in April 1996; acceptance of the mission would be a great boost to cosmology at MPA and throughout Europe. Cosmology within Germany was strengthened in a more modest way by a two-day joint meeting between the cosmology groups from the MPA and from the Astrophysikalisches Institut Potsdam. This brought together most of the active cosmologists in Germany and produced a very useful exchange of ideas. The next meeting of what should become a regular series is scheduled for Potsdam in Spring 1996.

When a new parallel supercomputer, intended for a small number of particularly computer-intensive projects, arrived at the RZG in September, MPA scientists were the only ones with production software ready to run simulations on the machine. As a result they got almost all the time in the first month of operation and the lion's share of it in the following month. The cover of this report shows an image from the first of these simulations. Although increased competition has reduced MPA usage to about the expected 20% level, this machine (and its larger successor) will clearly add substantially to the computational resources available to the institute.

1995 was also the first full year of operation of the Special Research Area ("Sonderforschungsbereich") dedicated to particle astrophysics, and a number of programmes are now underway in each of the three designated fields of research: experimental particle physics; theoretical particle physics and statistics; astrophysics and cosmology. MPA scientists are primarily active in the last area. A major initial goal was to enhance communication between the different participating institutions. A regular seminar series is underway, and a five day meeting of all interested scientists was held at Ringberg Castle in March. The latter even led to proceedings clad in a stylish black cover to emphasize the uniting thread of the search to identify the cosmic dark matter. Later in the year and on into 1996, each group in turn has been spending a day hosting scientists from the other institutions in order to present their programmes. The rumour is that after one year's work the nature of the dark matter is still uncertain!

1.4 How to reach us

- Postal address:

MPI für Astrophysik
Postfach 1523
85740 Garching
Germany

- Telephone (country code 49):

89-3299-00 (switchboard)
89-3299-3214 (secretary)
89-3299-3235 (FAX)

- Electronic address:

e-mail:
user-id@mpa-garching.mpg.de
(Initial + last name
will reach most people,
e.g. swhite for Simon White.)

World Wide Web:
http://www.MPA-Garching.
MPG.DE

anonymous ftp:
ftp.mpa-garching.mpg.de

2 Scientific Highlights

2.1 Turbulent diffusion in low-mass red giants

Stars begin their life converting hydrogen to helium by nuclear fusion in their centre. The Sun is presently in this phase. After the hydrogen supply has been used up, central hydrogen burning ceases, but the star can still shine because hydrogen fusion now takes place in a thin shell around the central helium core. The transition from central to shell burning is accompanied by large structural changes of the whole star. In particular, stars with a mass less than about $2 - 3M_{\odot}$ (solar mass) brighten and become larger but cooler at their surface. Stars in this phase are called "Red Giants". They also begin to transport the energy liberated in the hydrogen burning shell to the surface by means of mass flows known as "convection". Such convection mixes the stellar envelope thoroughly. After a star develops into a Red Giant, the convective outer regions extend to ever deeper layers of the star. At the same time its brightness (or "luminosity") increases and the surface (or "effective") temperature stays almost constant at about 3500 K. Plotted in a diagram showing the effective temperature of a star vs. its luminosity, Red Giants form an almost vertical line, the so-called Red Giant Branch (RGB). The increase in luminosity continues as the hydrogen shell advances, leaving behind the ashes of hydrogen fusion as a growing helium core. The high temperature of the burning shell stops the bottom of the convective envelope from getting too close, and eventually the transition point has to recede again. At its deepest point, however, the convective zone touches layers where a small fraction of hydrogen was processed to helium during the first stages of hydrogen core burning. As a result, convection can transport the products of hydrogen fusion to the visible layers of the star (its "photosphere").

Standard stellar evolution predicts that during this so-called first dredge-up the helium content in the envelope increases by a few per cent. This cannot be observed because of the low surface temperatures. However, some of this helium was produced via a nuclear cycle, in which four hydrogen nuclei (protons) are added to carbon, first converting it to nitrogen and then to oxygen. At the end of this "CNO-cycle", an oxygen atom reverts to carbon again by spitting out a helium atom. The CNO-cycle changes the relative abundances of the three heavy elements involved in a very characteristic way; specifically, a conversion of ^{12}C to ^{13}C and ^{14}N takes place, and the lines of these isotopes can very easily be observed. While the solar $^{12}C/^{13}C$ ratio is about 90, it is reduced to 4 in the CNO-cycle. Matter with this isotope ratio is transported to the surface by convection, but due to the dilution with virgin envelope matter, the photospheric value after dredge-up is predicted to be about 20–30. Similarly, the carbon abundance is reduced by about 30% and that of nitrogen increased by 80%. Oxygen and all other elements stay almost unchanged. These changes occur during the first dredge-up and after that episode the abundances are constant again for the rest of the RGB evolution.

Observations tell a different story: Panel a) of Fig. 2.1 illustrates that the carbon-to-iron abundance ratio, measured relative to that in the Sun and labelled [C/Fe] (defined as $\log(C/Fe)_{\star} - \log(C/Fe)_{\odot}$) is clearly decreasing with the absolute visual brightness M_v and therefore with time in red giants in the globular cluster M 92. The very low final C abundance of about 10% the solar one indicates that almost all carbon in the envelope must pass through regions hot enough for the CN-conversion while the stars evolve along the RGB. The same interpretation results from the middle panel (b), which shows (for stars in other globular clusters and

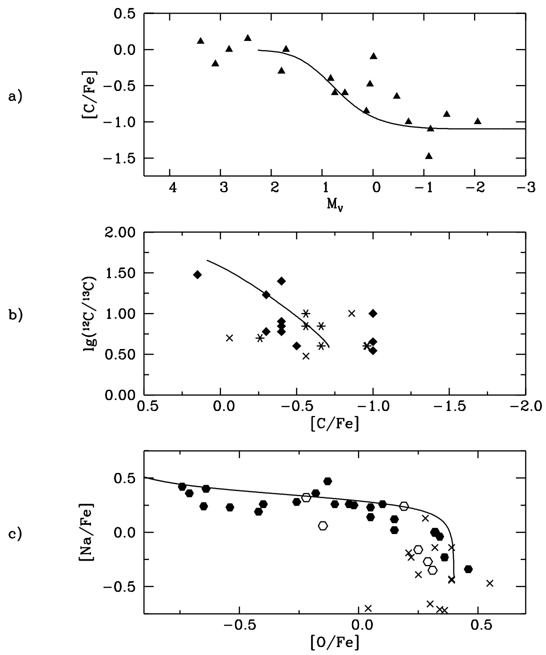

Figure 2.1: (a) The correlation of [C/Fe] with visual brightness in M 92; (b) the $^{12}C/^{13}C$ ratio for halo and globular cluster (M 4 and M 22) stars vs. carbon abundance; (c) the Na-O-anticorrelation found in globular cluster (M 3 and M 13) and field stars. Over the observational data (symbols) theoretical solutions applying additional diffusive mixing are plotted.

in the halo) that the $^{12}C/^{13}C$ ratio is decreasing from the value predicted by standard stellar evolution theory down to a value typical for the CNO-cycle. And finally, even heavier isotopes as sodium (Na), shown in panel c), display correlations (here with oxygen) which are expected only if matter from layers deep within the hydrogen burning shell is constantly being mixed to the surface; only at the high temperatures found inside the shell do the relevant processing cycles operate (e.g. neon-sodium and magnesium-aluminium cycles). The stars shown in Fig. 2.1 are all evolving up the RGB after the first dredge-up. Such isotope variations and anomalies are found in all globular clusters where they have been searched for. Apparently, some mixing process beyond the standard first dredge-up-scenario is operating in low-mass red giant stars.

Motivated by the idea that differential rotation between the bottom of the convective envelope and the top of the hydrogen burning shell might lead to turbulent diffusion between shell and envelope we have added diffusive mixing to our stellar models. It turns out that this process can very well reproduce the anomalies found (see Fig. 2.1), although the current models cannot produce the carbon and sodium anomalies in the same star. Presently, there is no object known which exhibits *both* anomalies, but if one should be found, the model would need to be extended.

In addition to the anomalies discussed so far, such turbulent diffusion models also explain oxygen isotope ratios measured in meteoretic grains that can be modelled neither with standard red giant nor with asymptotic giant evolution.

A final interesting question is the fate of ^{3}He in low-mass stars. In models which explain the carbon anomalies, ^{3}He which is produced in large quantities during core hydrogen burning and mixed into the envelope during the first dredge-up, is burnt very efficiently in the top layers of the hydrogen burning shell. The net effect by the end of red giant evolution is a strong depletion of ^{3}He compared to the initial abundance of the interstellar matter (ISM) out of which the star was formed. This is in severe conflict with standard stellar evolution, which predicts low-mass stars to be significant producers of ^{3}He, but it does lead to models for the chemical evolution of the galaxy, which are in agreement with the observational fact that the ^{3}He abundance in our Galaxy appears to have been constant over its entire evolution.

We still need proper physical models for the processes which produce diffusive mixing in the layers above the hydrogen shell. However, we are confident that our model correctly describes a mixing process, which is not contained in standard stellar evolution theory, but which manifests itself in the observed abundance anomalies. This process affects not only isotope anomalies in red giants, but also our understanding of the evolution of our Galaxy and of the synthesis of the light elements (e.g. ^{3}He) during the Big Bang. The latter can only be used to constrain the early evolution of our Universe if we have a good knowledge of how the observed light element abundances are affected by stellar processes. (Achim Weiss)

2.2 The Supersoft Sources

Supersoft Sources are a class of objects characterized by the emission of low-energy, or "soft" X-rays. The lack of any "hard" emission means that these sources were unobservable with the first X-ray telescopes and were first discovered by the EINSTEIN satellite just over a decade ago. Reliable data only became available with the ROSAT mission where the PSPC detector has a high sensitivity to soft X-rays.

Among the very different kinds of objects that show soft X-ray spectra we consider in the following only a new class of binary star which we refer to simply as Supersoft Sources (SSS). The peak of their spectrum is at an energy of 30 – 50 eV. Because of their short orbital periods, typically several hours, they must be close binary systems.

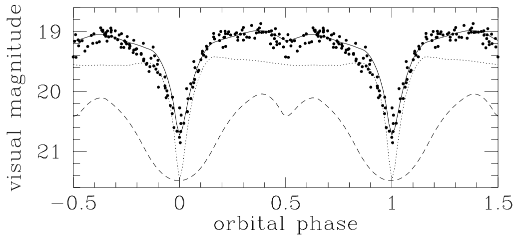

Figure 2.2: The diagram shows how the visual luminosity of CAL 87 (in magnitudes) depends on time over two orbital periods. The dots represent the observed light curve. The measurements were done between November 1985 and December 1992. The simulated total optical light curve (solid line) is the sum of the contributions of the star (dashed line) and of the disk (dotted line).

Close X-ray binaries consist of a compact object such as a white dwarf, a neutron star or a black hole and a secondary star comparable to our Sun. Generally, the size of the secondary is comparable to its Roche lobe which is defined as the surface which separates material which stays bound to the secondary from material which can escape and fall towards the compact primary star. The transferred gas forms an accretion disk in which viscosity causes the gas to spiral inwards while its angular momentum is transported outwards.

When matter accretes onto the compact star a large amount of energy is released and emitted as radiation. The smaller and more massive the accreting object, the more energetic the radiation. Accreting neutron stars, with a size of about 10 km, emit X-rays with energies mainly between 3 and 10 keV. Even if there were some additional structure, for example a large surrounding cocoon, their emitted radiation could not be much softer than this. Models based on accreting white dwarfs, roughly 1000 times larger than neutron stars, thus seem more promising for explaining the Supersoft Sources.

Soft X-rays are absorbed by interstellar gas in the plane of our Galaxy. Consequently, the first SSS were actually detected in the Magellanic clouds and the Andromeda nebula. Knowing the distance of these sources enabled their energy output to be calculated. It corresponds to the accretion of about 10^{-7} of the mass of the Sun every year. This is a very high rate compared to most X-ray binaries.

In similar binaries with lower accretion rates the transferred matter accumulates on the surface of the white dwarf until explosive nuclear burning of hydrogen starts. In this case the gas is expelled and the white dwarf gets much brighter. This so-called nova recurs on timescales longer than ten years. For higher accretion rates the intervals between subsequent nova outbursts get shorter. Hydrogen flashes occur. At accretion rates as large as observed in Supersoft Sources the hydrogen burning becomes steady. The resulting high luminosity of this nuclear process reproduces the unique X-ray properties of these binaries.

The orbits of some SSS are oriented so that disk and secondary star eclipse each other. In CAL 87 the visual brightness varies by almost two magnitudes (see Fig. 2.2). Analysing the spectrum of this source during eclipse of the disk by the secondary shows that the secondary makes a negligible contribution to the visible light. Thus the disk must be the main source at these wavelengths. However, a thin accretion disk, even if illuminated and heated by the X-rays from the white dwarf at its centre, is not bright enough to explain the observations. Furthermore, if the disk were thin, it should be possible to see the white dwarf directly, and one would then expect periodic X-ray eclipses which are not observed. The low ratio of X-ray to visual light in CAL 87 also suggests that some structure around the accretion disk may obscure the central X-ray source permanently.

An extended region, illuminated and heated by the white dwarf, can produce the observed high visual luminosity. Unlike other SSS where

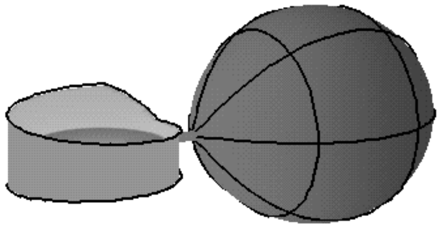

Figure 2.3: This figure illustrates a model for CAL 87. The Roche lobe filling secondary star (on the right) transfers matter to the white dwarf (hidden inside the accretion disk on the left). Note the asymmetric extended spray region around the disk generated by the interaction of a very massive accretion stream and the disk.

the X-rays from the white dwarf can be seen directly, the observed X-rays from CAL 87 are scattered, perhaps by a hot plasma wind of the kind observed around some SSS. The details of the observed optical and X-ray data confirm this hypothesis.

In CAL 87 the interaction of the massive accretion stream with the disk seems likely to produce an extended structure surrounding the disk near its outer edge. This interaction is supersonic and so shock waves are produced. Matter passing through the shocks is sprayed around almost explosively. Efficient cooling of the denser parts quickly leads to the formation of cold blobs and filaments. Embedded in the hot surrounding gas, this cold dilute matter takes part in the general Keplerian motion of the disk. The resulting toroidal structure is not axisymmetric (see Fig. 2.3) giving rise to the observed asymmetry in the visual light curve.

The emission of the disk and of the spray of gas can be calculated by assuming a black body radiation spectrum. Those parts facing the white dwarf are lit up and heated; the other parts remain cooler. The total emitted flux consists of the energy released by viscous dissipation in the disk and the reprocessed radiation of the white dwarf. The contribution of the secondary is composed of the original stellar flux and the reflection from that part of its surface which faces the X-ray source.

Figure 2.3 illustrates this model for CAL 87 and the solid line in Fig. 2.2 shows the calculated light curve. The depth of the primary minimum is fitted by an inclination of 77°. Thus the observer sees the system nearly edge-on. The illumination of the secondary increases its contribution to the visual emission mainly around orbital phase 0.5 where the heated part of the surface is visible to the observer. At this phase the secondary minimum indicates the partial eclipse of the star by the disk. The contribution of the disk is asymmetric as expected from the asymmetric spray geometry.

Several SSS have also been discovered in our Galaxy. For some of them the optical counterpart has been detected, and a few light curves have been measured. It will be interesting to see if the extended spray model which fits CAL 87 can also explain other Supersoft Sources. (Susanne Schandl)

2.3 The dynamics of wind accretion flows in massive X-ray binaries

High mass X-ray binaries are stellar systems consisting of a supergiant of 10 to 30 solar masses and a neutron star of about 1.5 solar masses. The supergiant, of spectral type O or B, emits a strong stellar wind which is propelled by radiation pressure. This driving mechanism is different from that of our Sun where pressure gradients are responsible for the wind. The mass loss rates associated with these stellar winds lie in the range (1 to 5) $\times 10^{-6}$ solar masses per year and reach velocities between 1000 and 2000 km/s at large distances. The X-ray emission of these systems is due to the material which the neutron star accretes from such a stellar wind. This material falls freely to the surface of the neutron star and emits there all its kinetic energy as X-rays. The observed X-ray luminosities of typically 10^{37} erg/s require a mass accretion rate of 10^{-9} solar masses per year. This is only a small fraction of the total mass loss rate. Theoretical models for wind accretion were first developed by Bondi and Hoyle. The accretion rates in these models are in good agreement with the values needed to explain the X-ray luminosities. This implies that the general model is correct. But there are still some unclear details of the mechanism which have been the subject of many studies in recent years.

Several groups have performed numerical calculations of such accretion flows. Earlier calculations were basically all two-dimensional be-

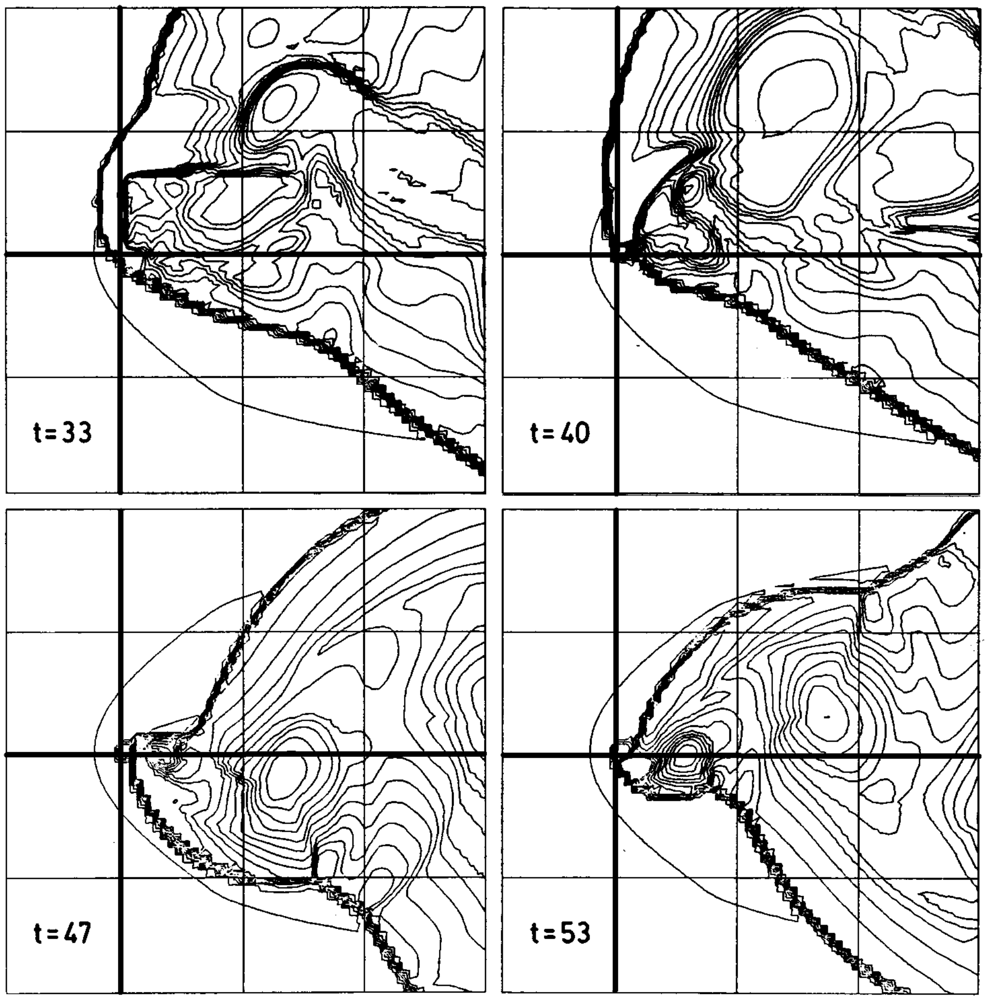

Figure 2.4: Density contours of a two-dimensional unstable accretion flow with Mach number $M_a = 3$ shown for four different times. The times are given in units of the flow travel time accross the whole field. The flow is from left to right and the accreting neutron star is located at the crossing of the bold orthogonal lines.

cause of the limitations of the computer capabilities. Since these flows are in general supersonic they develop a bow shock upstream from the accretor which then gives rise to the formation of a Mach cone. One finds that for sufficiently high numerical resolution these flows become unstable. They show so-called "flip-flop" instabilities in which this Mach cone moves from one side of the main stream direction to the other and back, as illustrated in Fig. 2.4. The instabilities disappear for low numerical resolution. The reason for this is that low resolution implies high numerical viscosity which damps the instabilities. Recently new and faster computers made it possible to calculate three-dimensional models with sufficiently high resolution. The instabilities obtained in these calculations are similar to those of two-dimensional models.

At present the physical mechanisms responsible for these instabilities are not yet fully understood. The instabilities can produce fluctuations in the accretion rates of mass and angular momentum. The observed X-ray sources pulsate due to the rotation of the magnetised neutron star, and so any accretion of angular momentum will result in a change of the pulse period. Therefore fluctuations in the rate of accretion of angular momentum will produce corresponding fluctuations in the change of the pulse period. This mechanism has been suggested to explain

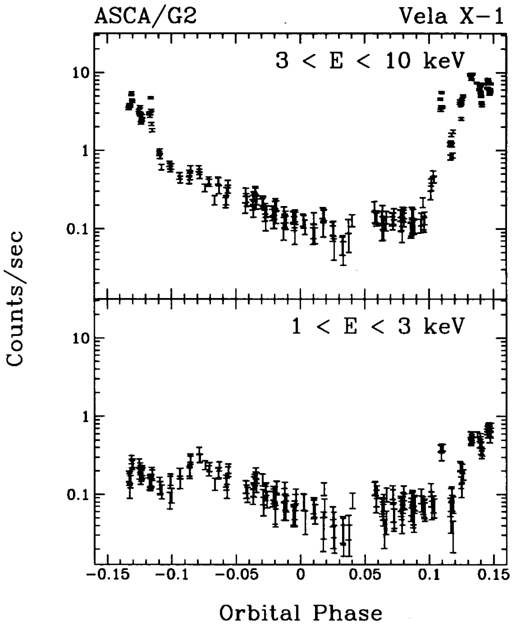

Figure 2.5: X-ray light curves of Vela X–1 obtained with the Japanese ASCA GIS2 detector in the energy bands 3–10 keV and 1–3 keV during the periods June 25–26 and July 5–6, 1993.

the observed random variation of the pulse period in these systems. But a careful analysis shows that the instabilities are about a factor ten too small to explain the observed fluctuations. Therefore a more complex accretion flow model has been developed which can give rise to fluctuations of the right magnitude. In this model angular momentum is temporarily stored in an accretion torus surrounding the magnetosphere of the neutron star.

Another very interesting aspect of such systems is the interaction of the X-rays with the stellar wind and its consequences for the dynamics of the wind. The most important effect of such a strong source of X-rays on the wind material is the ionisation of the gas. Since the wind acceleration occurs via UV line absorption which requires a low degree of ionisation, the gas in the neighbourhood of the X-ray source experiences only a very small acceleration force. In this region therefore only gravitational deceleration occurs. This means that the wind in a region around the neutron star will be much slower and therefore much denser than in regions which are not affected by the ionisation. Such a region of high density which trails the orbiting neutron star could be of importance in modelling asymmetric X-ray light curves. This type of asymmetric behaviour has been discovered recently in Vela X-1. The eclipse light curves (i.e. for the phases during which the X-ray source disappears behind the optical star) for the energy channels 1–3 keV and 3–10 keV are shown in Fig. 2.5. The high energy channel shows a sharp eclipse at phase −0.11 reducing the intensity by more than a factor ten. This is followed by a gradual decline from phase −0.11 to phase 0 by a factor of about 7. After this the intensity remains fairly constant until eclipse egress at phase 0.11. This long-lasting highly asymmetric behaviour of the light curve can only be explained by an extended high-density X-ray scattering region which trails the neutron star. Detailed models of stellar winds which have regions where the radiative driving force is switched off show that large enough regions of high density can be produced to be in agreement with the observations. Since it has turned out that the results depend strongly on the wind parameters assumed, we hope that the eclipse light curves will give us detailed information on the physics of the stellar winds in such binary systems. Similar asymmetries have recently been observed in spectral lines of HD 77581, the optical counterpart of Vela X–1. The fact that the sharp eclipses are not seen in the 1–3 keV channel indicates that here the optical depth is so large that the central X-ray source cannot be seen directly.

This short outline shows how much our knowledge of accretion flows in wind-fed X-ray binaries has increased over the recent years. It has become clear that such flows are intrinsically unstable and that the interaction of the X-ray ionisation with the stellar wind is of major importance. (Ulrich Anzer)

2.4 Protostellar accretion disks in T Tauri stars

T Tauri stars (see Fig. 2.6) are the late stages of star formation, and are often found in associations in the vicinity of molecular clouds. Spectroscopic studies reveal the central protostar (1 in Fig. 2.6) to be of low mass ($M \leq 2\mathrm{M}_\odot$). The continuum spectra of T Tauri stars show an infrared and ultraviolet excess which is generally interpreted as a circumstellar disk (2). The spectral shape indicates total disk masses between 0.001 and $1\mathrm{M}_\odot$. Doppler broadening in

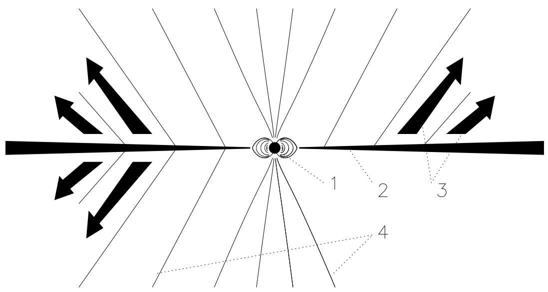

Figure 2.6: A schematic drawing of the late stage of star formation: a protostar (1) surrounded by an accretion disk (2) which is threaded by magnetic field lines (4). In the outer part of the disk we expect a disk–wind (3) launched along the magnetic field lines. At the inner edge of the disk the force of the dipole magnetic field of the protostar can dominate the hydrodynamic flow.

the observed line profiles (i.e., P Cygni profiles) is explained by copious mass loss in form of disk–winds (3). In several systems two collimated and outwardly expanding shells of gas and dust along the rotational poles are found. Measurements in molecular clouds, although ambiguous, suggest magnetic fields (4) to be dynamically important for the formation and evolution of T Tauri stars.

Stars form from molecular clouds by gravitational collapse. Besides pressure support these clouds are stabilized against gravity by rotation and by large-scale magnetic fields. However, the clouds are cold and the magnetic field lines connect only to ionized matter; they can diffuse through the neutral gas. Thus, a supercritical cloud fragment forms which collapses preferentially parallel to the rotation axis and along magnetic field lines. Rotation and the residual magnetic field prevent the cloud from being completely accreted by the protostar. Depending on the total angular momentum and the magnetic field strength, only a part of the cloud material falls onto the star. The rest forms an accretion disk around it. As the magnetic field is entrained in this collapse, it increases in strength and may become strong enough to support the disk partly against radial infall.

The last year has seen a concentrated effort to describe this disk phase of protostellar evolution, both analytically and numerically. This phase is interesting for various reasons. The cross–section of the disk is huge compared to that of the central star. Mass accreted from the molecular cloud therefore rains down preferentially onto the disk, rather than being accreted directly by the protostar. To build a theoretical understanding of the distribution of masses of newborn stars, it is essential to derive the fraction of the mass of the disk that is lost in the wind compared to the mass which ends up in the star. In addition, it is during this disk phase that planets form.

How can we model protostellar accretion disks? What are the physical ingredients which determine their structure? So far studies of protostellar accretion disks have neglected the dynamical importance of strong magnetic fields. Only the response of the disk to the tidal interaction of a companion star, or to the self-gravitation of the disk, was investigated. Are magnetic forces of crucial importance or do they just play a minor role for the evolution? To answer this question we wrote a computer code to study the hydrodynamic evolution of a thin magnetized accretion disk surrounding a central protostar. With this programme it is possible to study whether any chosen initial model for the disk is stable, or whether small perturbations grow and lead to a restructuring of the disk. By studying evolution from many different initial models, one can find out which kinds of disk configuration are stable.

The result of such a calculation is shown in Fig. 2.7. The initial magnetic field was maximal at 40% of the way to the outer disk edge, and it drops to zero at both disk edges. This magnetic field initially provided up to 15 per cent of the support of the disk against the protostar's gravitational force. After a short phase where the initial weak perturbation is growing ($t/T = 5$), a spiral arm develops ($t/T = 7$) and is followed by a phase of accretion ($t/T = 10$). This is seen in the evolution of the bright ring which moves inward with time. Subsequently, the excited waves damp out.

Results so far demonstrate that the evolution of protoplanetary disks can be strongly influenced by large–scale magnetic fields. There are two basic effects on the hydrodynamic flow. On the one hand an additional magnetic pressure increases the resistance against compression; on the other, different areas of the disk can be connented by arc–like magnetic fields extending through the magnetosphere. Differential rota-

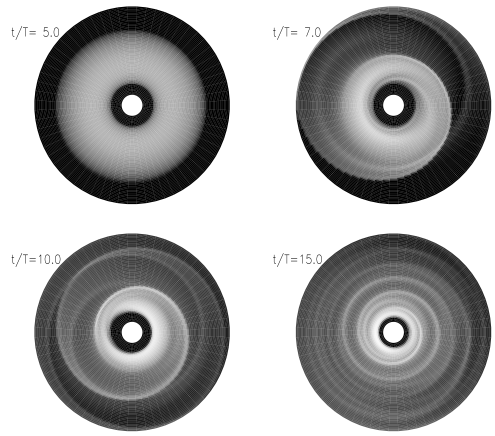

Figure 2.7: The time evolution of the surface density (white corresponds to high values) in a protostellar accretion disk. The time is in units of the orbital period at the outer edge of the disk. We observe a spiral perturbation to appear on a rather short dynamical timescale. After a phase of accretion, the excited waves damp out.

tion shears these magnetic field lines which then cause a redistribution of the disk gas. It appears that a one–arm spiral produces the strongest effects because it couples two disk areas over the widest radial range.

Even though many aspects of the evolution of magnetized accretion disks are still uncertain, it seems clear that many axisymmetric configurations become unstable against violent spiral instabilities when the magnetic field strength exceeds some critical limit. Guided by numerical studies like those described above, one can search for analytic models for these instabilities. The ultimate goal is a full description of a protostellar accretion disk including self–gravitation and mass loss through the wind. Such work should eventually set constraints on the conditions and timescale of the formation of planetary systems, a key–question closely connected to the uniqueness of mankind on the planet Earth. (Rudolf Stehle)

2.5 WZ Sge and the black hole connection

The galaxy is believed to contain a large number of black holes, formed by the collapse of massive stars during supernova explosions. There could be as many as 10^9 of them, with masses of typically a few solar masses. Most of these holes, black as they are, lead inconspicuous lives, and only under rare circumstances do they become visible.

The main evidence for their existence comes from X-ray binaries: double stars in which most of the radiation from the primary star is emitted as X-rays. In these stars, mass is transfered from an ordinary star (the secondary) to a compact object (the primary). If the primary star is small enough, the infalling gas gets hot enough to radiate in X-rays. In many cases, convincing evidence exists that the primary is a neutron star (this evidence comes mostly from observations of thermonuclear explosions taking place on the surface of the neutron star). Black holes as primaries, on the other hand are inferred from their *masses*. The mass of the primary is deduced, by Kepler's law, from the orbital period and the radial velocity of the secondary. If the lowest mass allowed by the observations is at least 3 solar masses, one calls the primary in an X-ray binary a 'black hole candidate' (BHC), since theoretical calculations predict that compact objects of mass larger than 2.5–3 solar masses must be black holes. In many ways the BHC's in our galaxy are like smaller copies of the nuclei of active galaxies (where massive black holes are suspected). For example, three BHC have now been found which produce jets moving at speeds close to the velocity of light, just like in active galaxies.

Some black hole candidates emit X-rays permanently (example: Cyg X-1), but most are transient sources that are visible in X-rays for only a month or so. They are discovered by X-ray observatories at a rate of 1–2 per year. Most have been seen only once, and are likely to repeat with periods more than a decade. They have a small companion which slowly transfers mass to the black hole. Instead of accreting steadily onto the hole (which would be seen as a steady X-ray flux), it appears that the mass gets stored for decades before getting dumped onto the hole during the transient. This storage is believed to take place in a disk or ring rotating around the hole. During this 'quiescent' phase almost no mass makes it to the hole, and the X-ray flux from the source is very low.

Observational evidence for such disks is found in several BHC, but the most detailed evidence comes from a related class of objects, the Cataclysmic Variables (CV's). These are very similar binaries, except that a white dwarf replaces the black hole in the center. They are much more numerous, and many of them close enough to Earth to allow detailed study of their accretion disks. Some of them show outbursts very similar to the black hole transients. The best studied of these is WZ Sge. It has shown outbursts (in visible light) in 1913, 1946, 1978, with a light curve very similar to that of a black hole transient: large amplitude, rapid rise, duration of the outburst several weeks. This similarity makes us suspect that the cause for the outbursts does not lie in the black hole or the white dwarf itself. Rather, it is believed that an instability in the disk storing the mass transferred from the secondary, is responsible for this behaviour. Models for such instabilities suffer from basic uncertainties about the properties of accretion disks. The most serious of these is the absence of a good theoretical model for the angular momentum transport in the disk. Usually this is taken to be some form of 'turbulent' viscosity, whose value is treated as an essentially free parameter, to be deterimined by some form of observational test. It has been shown over the past decade, in particular due to the work of Meyer and collaborators at our institute, that cyclic behaviour reminiscent of the outbursts in CV's results if this viscosity increases sufficiently rapidly with the temperature of the gas in the disk. A different mechanism causing outbursts was discovered by us, more or less by accident, in a full numerical simulation of the hydrodynamics in an accretion disk. This mechanism has nothing to do with turbulent viscosity: the simulations did not include viscous processes. Instead, it is due to a strongly nonlinear hydrodynamic instability, and causes angular momentum transport entirely through shock waves generated by the instability.

In both instability mechanisms the mass in the outer parts of the disk, which has been passively accumulating there during the quiescent phase, becomes active due to an increase in the efficiency of angular momentum transport. The difference lies in the different causes for this increase. It seems unlikely that improvements in theory will give us reliable models for either the unknown disk viscosity or the instability mechanism in the near future. Given this situation, we decided, in the project reported here, that guidance from new observations is necessary, and the object chosen for study was WZ Sge. Due to its proximity (200 light years, as opposed to the black hole transients which are typically 10 times further away), it can be studied in great detail. It also has the advantage that it is an eclipsing system: during its orbital motion, the secondary star partially eclipses the accretion disk, as seen from the Earth. Study of this eclipse can show us in detail (depending on the quality of the observations) what this disk looks like. Observations of WZ Sge were made with the Isaac Newton telescope on La Palma in July 1995.

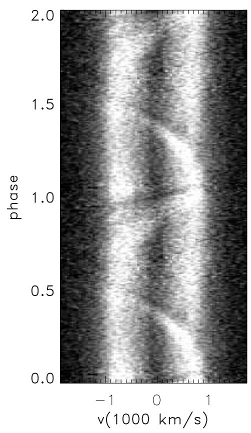

Figure 2.8: Variation with time of the H_α line profile of WZ Sge. Vertical axis is time (orbital phase of the binary), showing two orbits. Horizontal axis radial velocity (positive away from the observer).

The optical spectrum of WZ Sge (see Fig. 2.8) is very similar to that of a black hole transient source in quiescence. It is characterized by emission lines superposed on a continuum spectrum which is mostly due to emission by the white dwarf primary. The emission lines have a component that varies little with time (the two vertical stripes in Fig. 2.8), which is due to emission from the accretion disk. Since it is nearly axisymmetric, the disk looks the same from all directions presented to us during the orbital motion of the system, and so gives a time-independent line profile. In addition to this, there is a component whose observed wavelength varies sinusoidally with the orbital period, the so-called 'S-wave'. This is known to be the emission from the location on the outer disk (the 'hot spot') where the gas flowing from the secondary is heated by its impact on the disk. The eclipse of the disk by the secondary is seen as the inclined dark line near orbital phase 0. It confirms the rotation of the disk: the part of the disk coming towards us has blueshifted emission, and is eclipsed before the receding, redshifted part of the disk.

Quantitative analysis of the spectrum of Fig. 2.8 shows that there is cool gas orbiting the white dwarf down to almost the surface of the star. An unusual feature is the dark red-shifted 'shadow' to the right of the S-wave in Fig. 2.8, between phases 0.2 and 0.5. We interpret this as due to absorption of light from the hot spot by the disk. At those orbital phases when the hot spot is on the far side of the disk as seen from Earth, the line of sight from the hot spot shines through matter at the outer edge of the disk. The velocity difference causing the shift is due to the fact that the impacting stream causing the S-wave has a velocity which differs from the Keplerian motion of the disk. This feature gives a measure of the optical thickness of the outer region of the disk.

The gas seen in an emission line is optically thin in continuum radiation, and therefore not entirely representative of the bulk of the gas in the disk. The continuum radiation shows the denser parts of the disk. From the eclipse of the continuum the temperature and brightness of the disk, and the dependence of these quantities on distance from the primary can be determined. The next step is then the comparison of these results with theoretical models for the disk viscosity and the outburst mechanism. The standard outburst mechanism, for example predicts that a minimum temperature must be reached in the outer parts of the disk for an outburst to occur. The disk viscosity on the other hand is closely related to the disk's optical thickness. This work is in progress. (Henk Spruit)

2.6 Gamma-ray bursts – death throes of neutron star binary systems?

Roughly once a day gamma-ray detectors on Earth-orbiting spaceprobes like the Gamma Ray Observatory (GRO) register an intense flash of highly energetic electromagnetic radiation emanating from an unpredictable direction of the sky. The flashes brighten into visibility within typically a fraction of a second, last up to several hundred seconds, show random variations of intensity, and finally fade away so completely that no familiar celestial object has been found at the same place in the sky yet. If we had gamma-ray sensitive eyes the bursts would appear as bright as the full moon. Although they have been observed for over a quarter of a century now, these gamma-ray bursts remain as mysterious as when they were first seen in the late sixties.

Two key facts are considered as the clues to the distance from Earth of the objects that produce the bursts, namely isotropy and inhomogeneity. On the one hand, the positions at which the gamma-ray bursts appear on the sky seem completely isotropically distributed, and on the other hand, one observes very clearly a deficiency of weak bursts and thus a spatial inhomogeneity, implying that we can actually see the edge of the gamma-ray burster "cloud" surrounding us. These facts can be easily understood in the so-called cosmological models which place the bursters into the most distant parts of the Universe, billions of light years away. Isotropy and inhomogeneity follow naturally from that assumption: We are at the center of the observable Universe, and the volume we get information from is finite.

In order to cause the gamma-ray brightness measured in the detectors, the objects that produce the bursts at cosmological distances must release an enormous amount of energy within a short time, namely roughly the energy the Sun will radiate during its whole lifetime! Even more, due to the variability of the gamma-ray flux on timescales of milliseconds to seconds, the volume in which this energy is generated and released has to be extraordinarily small, roughly 100 km. Only processes involving very compact astrophysical objects like neutron stars or black holes have a chance to meet these requirements.

The catastrophic end of a double neutron star or a binary system of a neutron star and a black hole is currently the most popular idea for the possible origin of the enigmatic gamma-ray bursts. One argument in favor of this suggestion is based on the merger rate. From the number of binary star systems and the theoretical knowledge about binary star evolution, one estimates with the huge number of galaxies in the visible Universe that the number of merging events per day could well be large enough to account for the detected gamma-ray burster rate. Thus, the association of neutron star mergers with gamma-ray bursts would automatically place the latter to cosmological distances. Another argument in favor of this association is the enormous amount of gravitational binding energy that is set free

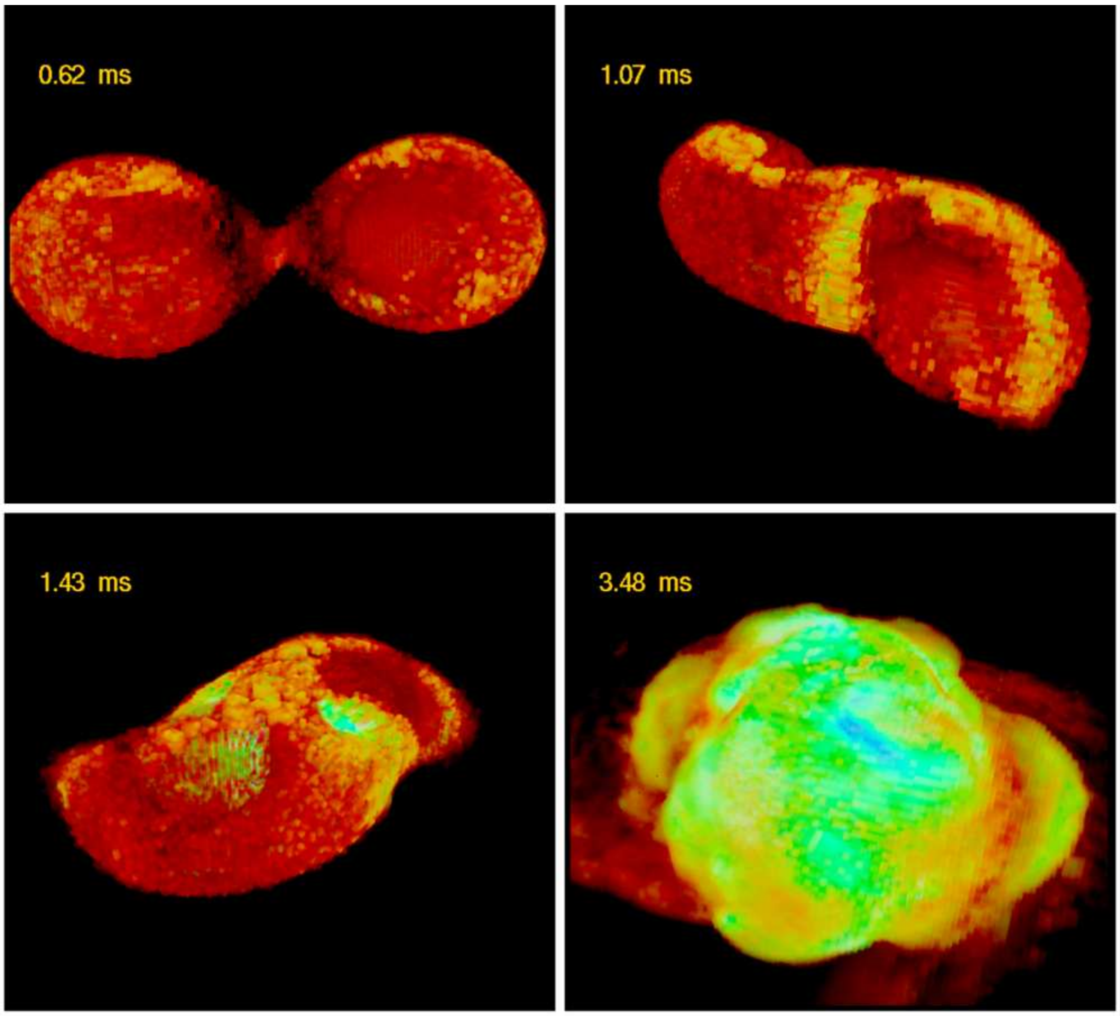

Figure 2.9: Four snapshots of the merging of two neutron stars. The sequence of events runs from the top left to the top right, lower left, and lower right panel. The times given in the upper left corner of each panel are measured in thousandths of a second (from the beginning of the simulation) which is roughly the orbital period of the binary system. The pictures show that the final, dynamical interaction and coalescence of the two neutron stars happens within a tiny fraction of a second. The merging is visualized like a close observer would "see" it in the "neutrino light". Red color means relatively low temperature in the neutrino emitting region, yellow, green, light blue, and dark blue indicate successively higher temperatures.

during the coalescence of binary neutron stars.

It was the aim of the work described in this article to develop exact numerical models for the dynamical merging of neutron star binary systems in order to put the suggested mechanism for the transformation of the released energy into high-energy photons to a quantitative test. To this end, we have performed three-dimensional hydrodynamical simulations of the final stages of the binary evolution and of the dynamical coalescence of two identical neutron stars. These are the first detailed numerical models that were obtained with a physical high-density equation of state and that include the effects due to the production of elementary particles like neutrinos in the hot neutron star matter. The emission of gravitational waves and the corresponding back-reaction on the hydrodynamical flow by energy and momentum loss were also taken into account.

During the merging, the initially cold or cool neutron stars heat up strongly and their interior temperatures reach more than 100 billion degrees, or, in energy units, several 10 Megaelectronvolts (MeV). At such extreme conditions, extremely high temperatures combined with densities close to and even above nuclear matter density, reactions between protons, neutrons, electrons, and positrons, the antiparticles of electrons, produce huge numbers of neutrinos and antineutrinos. Although (anti)neutrinos interact only very weakly with matter — their interaction probability is about 20 orders of magnitude smaller than that of photons — they cannot escape immediately and unhindered because hot neutron star matter is very opaque against neutrinos. Nevertheless, since photons are so much more tightly coupled to the stellar matter, neutrinos, besides gravitational waves, are the main direct leak of energy from the merger.

Figure 2.9 displays color-coded images of the time evolution of the neutron star merging as it would be seen in neutrino "light". Red color denotes comparatively "cool" emission of neutrinos with mean energies below about 6 MeV. Yellow corresponds to 9–12 MeV mean neutrino energy, green to 15–18 MeV, cyan to 21–24 MeV, and blue denotes emission of neutrinos with at least 27 MeV average energy from the regions of highest temperatures. The sequence of snapshots demonstrates how the neutron stars heat up and their surfaces attain higher and higher temperatures. The gas temperatures in the emitting regions are roughly one third of the mean neutrino energies. The upper left panel shows the situation when the surfaces of the two neutron stars come into contact first at 0.62 thousandths of a second after the start of the simulation. Tidal forces stretch the neutron stars and create a bridge of matter between the approaching stars. In the upper right panel (time 1.07 ms) the stellar surfaces touch each other and the neutron stars begin to fuse while shearing motions heat up their common interface. The panel on the lower left (time 1.43 ms) displays the object shortly after merging. Elongated, curved, arm-like structures are caused by centrifugal forces on the opposite, outer sides. These "wings" become more extended as time goes on (lower right panel at time 3.48 ms). They are heated and dispersed into an inhomogeneous "ring" of matter by the interaction with pressure waves caused by the wobbling and swinging of the central, hot core of the merged object which can be seen in cyan and blue colors.

The direct photon or gamma-ray flux from the merger is negligibly small because the matter is extremely opaque to photons. However, emitted neutrinos can annihilate with their corresponding antineutrinos with a certain probability to form a cloud of electron-positron pairs in the surroundings of the merged object. In subsequent reactions between electrons and positrons, photons with very high energies are produced. The relativistically expanding fireball of electron-positron pairs and photons was suggested to be the source of the detected gamma-ray bursts.

Contrary to these expectations, our simulations reveal that — although the neutrino emission becomes extremely luminous shortly after the neutron stars have merged — the probability of neutrino-antineutrino interactions is too small and the phase of high neutrino emission too short to pump enough energy into the fireball to account for gamma-ray bursts at cosmological distances. The central, compact object formed in the merger (cyan and blue colors in the lower right panel of Fig. 2.9) has about three times the mass of the Sun and is therefore so massive that it can neither be stabilized by internal pressure nor by rotation. Thus, it will inevitably collapse into a black hole within a few thousandths of a second. If all matter falls into the black hole directly, the neutrino fluxes are quenched almost immediately. However, our models suggest that some of the more dilute material that surrounds the central body (red and yellow regions in the lower right panel of Fig. 2.9) has sufficiently large angular momentum that it might remain in a disk around the black hole for some while. This material could therefore be accreted into the black hole on a much longer timescale during which it would copiously radiate neutrinos. Unfortunately, analytical considerations lead to the same conclusion as our numerical simulation of the dynamical merging phase: Even under the most favorable conditions, the energy provided by annihilation of neutrinos and antineutrinos emitted from the disk falls short by nearly two orders of magnitude and thus cannot account for cosmological gamma-ray burst events.

Certainly, this result is rather disappointing. Nevertheless, the described quantitative investigations and simulations have very important implications, because they strongly emphasize that the enigmatic gamma-ray bursts cannot be explained by neutrino annihilation in the vicinity of merging binary neutron stars. The currently most popular idea fails to solve the puzzle. Therefore more complicated models have to be considered, possibly involving effects of amplified and very strong magnetic fields in the merger. Also completely different types of scenarios have to be taken more seriously. (Maximilian Ruffert & H.-Thomas Janka)

2.7 Simulations of relativistic jets

In 1918 H.D. Curtis photographed the giant elliptical galaxy M87 and noticed a "curious straight ray", which was "apparently connected with the nucleus of the galaxy by a thin line of matter". This was the first discovery of a so–called extragalactic jet. Nowadays several hundreds of these extragalactic jets are known. Most of them were discovered by radio observations, because they seem to transport enormous amounts of energy from the nuclei of radio galaxies and quasars (point–like quasi–stellar radio sources emitting enormous amounts of energy) to intergalactic space, thereby powering the extended regions of radio emission (the so–called radio lobes) of these sources. High resolution radio interferometry has shown that the jets are extremely well collimated extending from the very centre of the galaxy all the way out to distances of several hundred thousand light years.

Besides the extragalactic jets, one has also found collimated outflows in some galactic binary systems, most notably in the binary star SS433. The stellar jet of SS433, which was discovered in the late seventies, propagates with a velocity equal to one quarter of the speed of light, i.e., its velocity is near–relativistic. Even larger jet speeds have recently been observed for two galactic X-ray sources, which consist of binaries where one member of the binary is most likely a black hole. The measured apparent (transverse) motion for both sources exceeds the speed of light. This phenomenon, commonly referred to as "superluminal" motion, is also observed for many extragalactic jets at distances of light years up to a few thousand light years. Superluminal motion is widely interpreted as the result of highly relativistic bulk velocities, which are oriented nearly along to the line of sight. For a source of radiation moving near the speed of light the apparent time duration between two events seen by a distant observer is compressed if the motion is close to the line of sight, because the source "chases" its own radiation. Hence, the apparent velocity of the projected motion on the sky can appear to exceed the speed of light.

Recent observations of the quasar 3C31 show that the speed of its jet decreases significantly with increasing distance from the centre. This observed "slow down" of an initially relativistic jet has led some researchers to argue that probably *all* extragalactic jets propagate at relativistic speeds, at least close to the source.

Because of this observational evidence, we have begun to perform simulations of relativistic jets. Such simulations were not feasible until a few years ago when appropriate numerical methods were developed, because the relativistic equations are substantially more complicated and harder to solve than the non–relativistic ones. In our simulations we assumed (as in most other studies) that the gas pressure in the jet is equal to the pressure exerted by the ambient gas (pressure–matched jets), which seems to be roughly the case in astronomical jets.

Our studies revealed that relativistic jets show the same main features as non–relativistic ones (Figs. 2.10 and 2.11). A supersonic *beam* of nearly constant diameter, which periodically slightly expands and converges. This causes a series of internal oblique shock waves, which collimate the flow. The supersonic flow terminates